BMC Pharmacology and Toxicology

RESEARCH Open Access

Nociceptive transient receptor potential ankyrin 1 (TRPA1) in sensory neurons are targets of the antifungal drug econazole

Kaoru Kasuya[1], Kenji Takahashi[1,2], Miho Hashimoto[2] and Toshio Ohta[1,2*]

Abstract

Background Econazole is a widely used imidazole derivative antifungal for treating skin infections. The molecular targets for its frequent adverse effects of skin irritation symptoms, such as pruritus, burning sensation, and pain, have not been clarified. Transient receptor potential (TRP) channels, non-selective cation channels, are mainly expressed in peripheral sensory neurons and serve as sensors for various irritants.

Methods We investigated the effect of econazole on TRP channel activation by measuring intracellular calcium concentration ($[Ca^{2+}]_i$) through fluorescent ratio imaging in mouse dorsal root ganglion (DRG) neurons isolated from wild-type, TRPA1$^{(-/-)}$ and TRPV1$^{(-/-)}$ mice, as well as in heterologously TRP channel-expressed cells. A cheek injection model was employed to assess econazole-induced itch and pain in vivo.

Results Econazole evoked an increase in $[Ca^{2+}]_i$, which was abolished by the removal of extracellular Ca^{2+} in mouse DRG neurons. The $[Ca^{2+}]_i$ responses to econazole were suppressed by a TRPA1 blocker but not by a TRPV1 blocker. Attenuation of the econazole-induced $[Ca^{2+}]_i$ responses was observed in the TRPA1$^{(-/-)}$ mouse DRG neurons but was not significant in the TRPV1$^{(-/-)}$ neurons. Econazole increased the $[Ca^{2+}]_i$ in HEK293 cells expressing TRPA1 (TRPA1-HEK) but not in those expressing TRPV1, although at higher concentrations, it induced Ca^{2+} mobilization from intracellular stores in untransfected naïve HEK293 cells. Miconazole, which is a structural analog of econazole, also increased the $[Ca^{2+}]_i$ in mouse DRG neurons and TRPA1-HEK, and its nonspecific action was larger than econazole. Fluconazole, a triazole drug failed to activate TRPA1 and TRPV1 in mouse DRG neurons and TRPA1-HEK. Econazole induced itch and pain in wild-type mice, with reduced responses in TRPA1$^{(-/-)}$ mice.

Conclusions These findings suggested that the imidazole derivatives econazole and miconazole may induce skin irritation by activating nociceptive TRPA1 in the sensory neurons. Suppression of TRPA1 activation may mitigate the adverse effects of econazole.

Keywords Antifungal, Heterologous expression, Intracellular Ca^{2+} concentration, Nociceptor, Sensory neuron, Transient receptor potential channel

*Correspondence:
Toshio Ohta
tohta@tottori-u.ac.jp
[1]Department of Veterinary Pharmacology, Faculty of Agriculture, Tottori University, Tottori 680-8553, Japan
[2]Department of Veterinary Pharmacology, Joint Graduate School of Veterinary Sciences, Tottori University, Tottori 680-8553, Japan

Background

Econazole is a broad-spectrum imidazole antifungal agent that is primarily used for treating dermatophyte infections, such as tinea pedis and ringworm. It is typically administered topically in the form of a cream. Although many patients experience a favorable cure rate of 90%, 1–4% of individuals may encounter side effects, such as pruritus, burning sensation, and erythema [1, 2].

Pain and itching are uncomfortable sensations that arise through complex pathways involving afferent sensory neurons in peripheral tissues, such as the skin. Various types of transient receptor potential (TRP) channels serve as nociceptors, which respond to chemical, thermal, and mechanical stimuli to evoke sensations of pain and itching [3]. Among these channels, TRPV1 and TRPA1 play essential roles in nociception [4]. As nonselective cation channels in sensory neurons, their activation in peripheral terminals results in the entry of Ca^{2+} and Na^{+}, leading to membrane depolarization and the generation of action potentials. These action potentials transmit sensory information to the spinal cord and, subsequently, to higher nerve centers [5, 6].

Although the concept of TRPA1 functioning as a cold sensor in mammals remains a topic of debate [7], this channel is well-known for its responsiveness to various chemical stimuli, such as cinnamaldehyde and mustard oil [8]. In contrast, TRPV1 channel is recognized as a receptor for pungent compounds, such as capsaicin, as well as acidic pH and heat [9, 10]. Notably, some medications that are currently in use can stimulate nociceptive TRP channels. For instance, the widely used local anesthetic lidocaine activates both TRPA1 and TRPV1, leading to the sensation of pain [11, 12]. Flufenamic acid, which is a nonsteroidal anti-inflammatory drug (NSAID), has been reported to activate TRPA1 [13], and several NSAIDs have been linked to skin irritation [14, 15]. Propofol, which is an intravenous general anesthetic, induces intense vascular pain by activating TRPA1 [16]. Furthermore, retinoid, which is commonly used in the treatment of skin disorders, has been found to sensitize TRPA1 and cause skin irritation [17]. These studies collectively suggest the association of TRP channel activation with the adverse effects of skin irritation by certain medications.

In this study, we aimed to investigate the involvement of TRPA1 and TRPV1 channels in econazole-induced skin irritation using analytical techniques, such as calcium imaging, along with pharmacological and genetic approaches. We also investigated whether econazole causes itch and pain behaviors using cheek injection model. Moreover, to understand the structural specificity of econazole, we examined the activities of miconazole, which is another imidazole antifungal drug, and the triazole antifungal drug fluconazole.

Methods

Experimental animals

All experimental protocols on animals were approved by the Committee on Animal Experimentation of Tottori University. The number of animals used was minimized.

Isolation and culture of mouse DRG neurons

We used adult (4–12-week-old) C57BL/6 mice [wild type, $TRPA1^{(-/-)}$, and $TRPV1^{(-/-)}$] of either sex. The $TRPA1^{(-/-)}$ mice were kindly provided by Dr. Julius of the University of California, whereas the $TRPV1^{(-/-)}$ mice were purchased from Jackson Lab (Sacramento, CA, USA).

Euthanasia was administered to the mice by CO_2 gas inhalation. Mouse dorsal root ganglion (DRG) cells were isolated and cultured, as described previously [18]. In brief, DRGs were removed and minced in phosphate-buffered saline (PBS: 137 mM NaCl, 10 mM Na_2HPO_4, 1.8 mM KH_2PO_4, and 2.7 mM KCl). Thereafter, the DRGs were enzymatically digested for 30 min at 37 °C in PBS containing 1 mg/ml of type II collagenase (Worthington, Lakewood, NJ, USA) and 1 mg/ml of DNase I (Roche Molecular Biochemical, Indianapolis IN, USA). Subsequently, the DRGs were further digested in PBS containing 10 mg/ml of trypsin (Sigma, St. Louis, MO, USA) and 1 mg/ml of DNase for 15 min at 37 °C. The digested ganglia were immersed in Dulbecco's modified Eagle medium (Sigma) supplemented with 10% fetal bovine serum (BioSera, Cholet, France), penicillin G (100 U/ml), and streptomycin (100 μg/ml). DRG cells were obtained by gentle trituration using Pasteur pipettes. The cell suspension was centrifuged at 800 rpm for 2 min at room temperature, and the pellet was resuspended in the culture medium. Aliquots were placed onto glass cover slips coated with poly-D/L-lysine (Sigma) and cultured in a humidified atmosphere of 95% air and 5% CO_2 at 37 °C. The cells were used within 24 h after the isolation.

Heterologous expression in HEK293 cells

Human embryonic kidney (HEK) 293 cells were maintained in the culture medium, as described above. The cells were transfected with the expression vectors (mouse TRPA1 and mouse TRPV1) [18] using a transfection reagent (Lipofectamine 2000, Invitrogen, Tokyo, Japan), according to the manufacturer's protocol, and used within 24 h after transfection.

Calcium imaging

The intracellular Ca^{2+} concentrations ($[Ca^{2+}]_i$) in the individual cells were measured using a fluorescent-imaging system (Aqua Cosmos, Hamamatsu Photonics, Japan), as described previously [19]. Briefly, the cells were incubated for 40 min at 37 °C with 10 μM fura-2 AM (Molecular Probes) in HEPES-buffered solution

(134 mM NaCl, 6 mM KCl, 1.2 mM $MgCl_2$, 2.5 mM $CaCl_2$, 10 mM glucose, and 10 mM HEPES; pH 7.4). A coverslip with fura-2-loaded cells was transferred into an experimental chamber and mounted on an inverted microscope (Olympus IX71), which was equipped with image acquisition and analysis system. The cells were illuminated every 5 s with light at 340 and 380 nm, and the respective fluorescence signals at 500 nm were detected. The ratios of fluorescent signals (F340/F380) were analyzed. Calibration of fura-2 was carried out with standard Ca^{2+} buffer solutions (Calcium Calibration Buffer Kits, Invitrogen) containing 4 μM fura-2 (Invitrogen) with the equation reported by Grynkiewicz et al. [20]. The cells were continuously superfused with an external solution at a flow rate of approximately 2 ml/min by gravity. Drugs were applied by replacing the reflux tube with a test tube containing the drug in the HEPES-buffered solution. The 80 mM KCl solution included 80 mM KCl, 60 mM NaCl, 1.2 mM $MgCl_2$, 2.5 mM $CaCl_2$, and 10 mM HEPES. For the Ca^{2+}-imaging experiments, regions of interest (ROIs) were set on spherical, neuron-like cells. Consequently, almost all selected cells responded to 80 mM KCl. Cells with significantly high resting $[Ca^{2+}]$i or cells that were evidently dead were excluded from the analysis. All experiments were carried out at room temperature (22–25 °C).

Behavioral test

A cheek injection model was used to determine econazole-induced itch and pain using male wild type and $TRPA1^{(-/-)}$ mice (8–14 weeks old). After a 30 min habituation, 10 μl of vehicle or econazole (20 nmol) was intradermally injected into the right cheek of the mice with a 30-gauge needle syringe (BD Lo-Dose, Becton Dickinson, Fukushima, Japan). Behaviors were recorded for 30 min with a digital camera (HDR-PJ40V, Sony, Tokyo, Japan). Scratching and wiping behaviors directed toward the injection site were counted, and the former and latter was judged as itch and pain, respectively [21, 22].

Chemicals

The following drugs were used as vehicle and concentration for stock solution: allyl isothiocyanate (AITC) in 1 M dimethyl sulfoxide (DMSO) (Nakarai, Tokyo, Japan); capsaicin (Cap) in 1 mM ethanol (Sigma-Aldrich); A967079 in 0.01 M DMSO (Santa Cruz); N-(4-t-butylphenyl)-4-(3-chloropyridin-2-yl) tetrahydropyrazine-1(2 H)-carboxamide (BCTC) in 5 mM DMSO (Wako); and econazole, miconazole, and fluconazole, each in 0.1 M DMSO (Tokyo Chemical Industry, Tokyo, Japan); thapsigargin in 0.01 M DMSO (Wako). All the other drugs used were obtained from Wako.

Data analysis

The data are presented as mean ± SEM (n = number of cells). Comparison between two groups was performed by unpaired Student's *t*-test. For multiple comparisons, one-way analysis of variance followed by the Tukey–Kramer test or Steel-Dwass test was used. A P value of <0.05 was considered statistically significant.

Results

$[Ca^{2+}]_i$ response to econazole in mouse DRG neurons

In Fig. 1A, we present the chemical structures of the three antifungal drugs used in the present study. Because nociceptive TRP channels are known for their high Ca^{2+} permeability [23], we used calcium imaging to examine the effects of econazole on $[Ca^{2+}]_i$ in mouse DRG neurons. Econazole elicited $[Ca^{2+}]_i$ increases in mouse DRG neurons that were responsive to 80 mM KCl (Fig. 1B). The amplitude of the $[Ca^{2+}]_i$ and the percentage of neurons responding to econazole increased in a concentration-dependent manner (Fig. 1C, D). High concentrations of econazole seem to evoke Ca^{2+} release from intracellular stores (see in Fig. 3). To determine whether stored Ca^{2+} depletion was related to the saturation of $[Ca^{2+}]_i$ responses, we examined the effect of thapsigargin, an inhibitor of endoplasmic reticulum Ca^{2+}-ATPase, which leads the depletion of intracellular stored Ca^{2+} [24]. There was no difference in the magnitude of the response of econazole (100 μM) between thapsigargin (1 μM)-treated and -untreated cells (treated: 98.0 ± 5.2 nM, $n=95$; untreated: 91.2 ± 4.0 nM, $n=88$). Notably, econazole at 100 μM increased the $[Ca^{2+}]_i$ in nearly all neurons and suppressed the $[Ca^{2+}]_i$ responses to the subsequently applied KCl (Fig. 1B and C). These findings suggested that econazole stimulated sensory neurons, but it also exhibited nonspecific effects at high concentrations. Consequently, in the following experiments, we analyzed the effects of econazole at concentrations of 10 and 30 μM.

Next, we investigated the effect of removing extracellular Ca^{2+} on the econazole-induced responses. Removal of extracellular Ca^{2+} completely eliminated the econazole-induced increase in the $[Ca^{2+}]_i$ (Fig. 1E, F). These results indicated that the $[Ca^{2+}]_i$ responses to econazole at 10 and 30 μM were solely dependent on the influx of extracellular Ca^{2+}.

Relationships between responsiveness to econazole and TRP channel agonists in mouse DRG neurons

TRPA1 and TRPV1 are nonselective cation channels that are permeable to calcium, expressed in DRG neurons, and involved in pain and itch signaling [3]. We aimed to investigate the econazole sensitivity of a subpopulation of neurons expressing TRPA1 and/or TRPV1. Since TRP channel activators often elicit channel desensitization

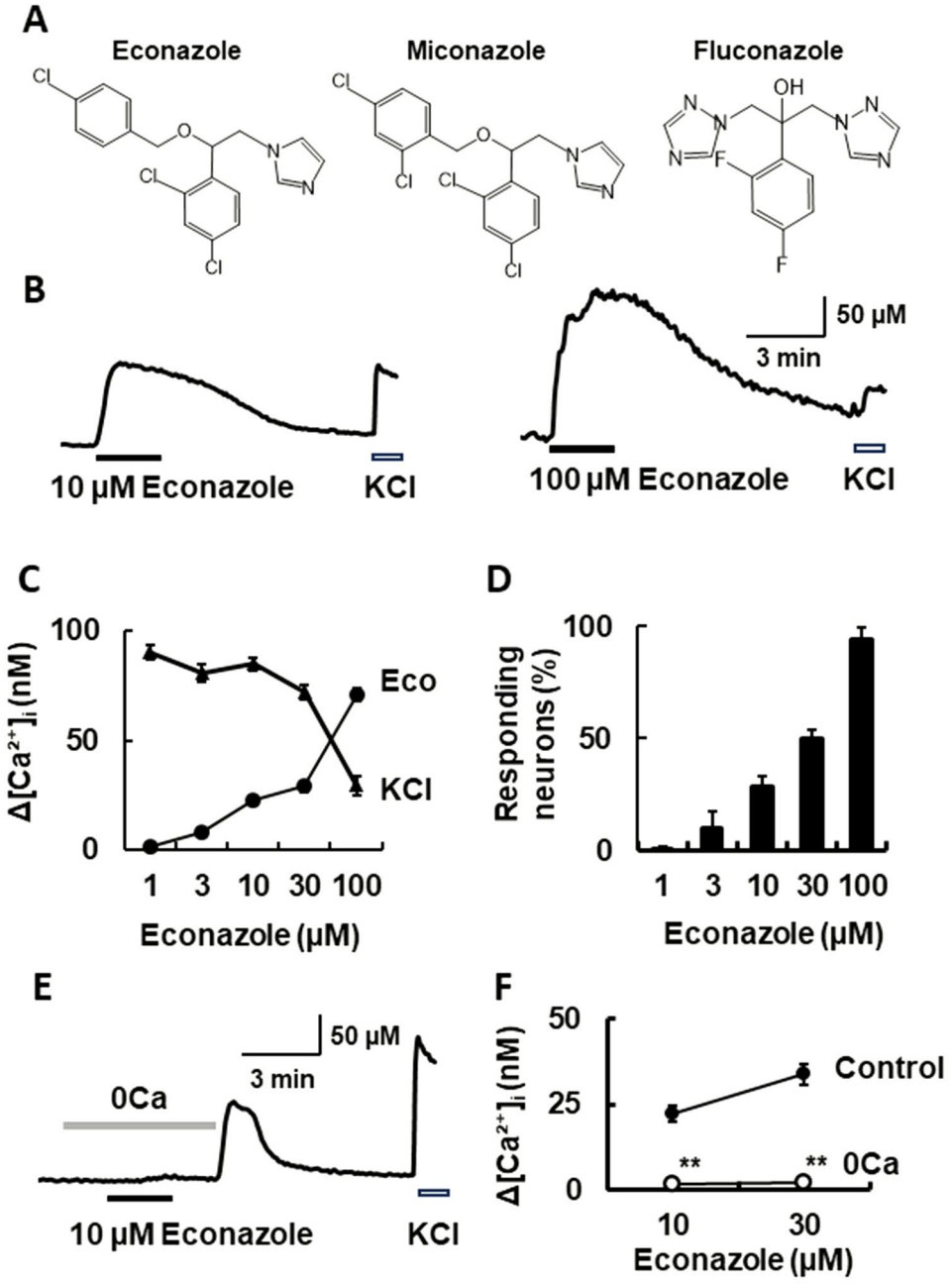

Fig. 1 Econazole-induced changes in $[Ca^{2+}]_i$ in mouse DRG neurons. (**A**) The chemical structures of econazole, miconazole, and fluconazole are shown. (**B**) The actual recordings of $[Ca^{2+}]_i$ responses to econazole at 10 μM (left) and 100 μM (right) and to 80 mM KCl in wild type mouse DRG neurons. (**C**) The relationship between the magnitude of $[Ca^{2+}]_i$ increase induced by econazole (Eco) and by KCl at different concentrations of econazole. (**D**) The percentages of the neurons responding to econazole at various concentrations are shown. Symbols or columns with vertical lines represent the mean values ± SEM for each econazole concentration ($n = 193–395$ from 4–6 mice). (**E**) The actual recording of $[Ca^{2+}]_i$ responses to 10 μM econazole in the absence of external Ca^{2+} (0Ca) and KCl is shown. The 0Ca period is indicated with a grayish bar. (**F**) A summary of the amplitudes of $[Ca^{2+}]_i$ responses to econazole at 10 and 30 μM in the presence (control) and absence of extracellular Ca^{2+} (0Ca) ($n = 133–190$ from three mice) is shown. $^{**}P < 0.01$ vs. control, as determined by Student's t-test

[25], mouse DRG neurons were applied with econazole first, followed by the selective agonists for TRPA1 (i.e., AITC, 100 μM) and TRPV1 (i.e., capsaicin, 1 μM). This order was adopted so that the TRP agonists would not affect the action of econazole. The same protocol was done with miconazole and fluconazole, which are described later. Some of the econazole-sensitive neurons responded to AITC and/or capsaicin (Fig. 2A). The Venn diagram in Fig. 2B illustrates the characteristics of all neurons. Many neurons responded to both

AITC and capsaicin, likely because a significant number of neurons coexpress TRPA1 and TRPV1 [26]. At 10 μM of econazole, almost all of the econazole-sensitive neurons responded to AITC (n=35, 94.6%), and a subset responded to capsaicin (n=22, 59.5%). Of the DRG neurons that responded to 30 μM of econazole (n=67), some were sensitive to AITC (n=27, 40.2%) and capsaicin (n=34, 50.7%). Moreover, the neurons that did not respond to either AITC or capsaicin responded to 30 μM of econazole (n=28, 41.8%). These results suggested that econazole at 10 μM primarily increased $[Ca^{2+}]_i$ in the DRG neurons expressing TRPA1; at 30 μM, it can also affect a different subset of neurons expressing molecules other than TRPA1 and TRPV1.

Effect of pharmacological and genetic inhibition of TRPA1 and TRPV1 on econazole-induced stimulation in mouse DRG neurons

Because econazole increased $[Ca^{2+}]_i$ in neurons that were sensitive to TRP channel agonists, we examined the effect of pharmacological inhibition on the $[Ca^{2+}]_i$ responses to econazole in mouse DRG neurons. Application of the TRPA1 antagonist A967079 (10 μM) significantly suppressed the $[Ca^{2+}]_i$ responses to econazole at 10 μM but not at 30 μM. Conversely, treatment with selective TRPV1 antagonist BCTC (10 μM) failed to inhibit the $[Ca^{2+}]_i$ responses to econazole (Fig. 2C).

We further assessed the effect of genetic depletion of TRPA1 and TRPV1 on the econazole-induced $[Ca^{2+}]_i$ responses using knockout mouse DRG neurons. As shown in Fig. 2D, the econazole-induced responses were significantly diminished, although only slightly at 30 μM, in the $TRPA1^{(-/-)}$ mouse DRG neurons. In contrast, the magnitudes of the $[Ca^{2+}]_i$ responses to econazole in the $TRPV1^{(-/-)}$ mouse DRG neurons were not significantly reduced, compared with those in wild type neurons.

These results suggested that econazole selectively activated the TRPA1 channels at 10 μM and may interact with other molecules at higher concentrations, leading to Ca^{2+} influx in mouse DRG neurons.

Effect of econazole on heterologous TRPA1-expressing cells

To further investigate the stimulatory action of econazole on TRPA1, we evaluated its effects on HEK293 cells with heterologous expression of TRPA1 (TRPA1-HEK). Based on our findings on nonspecific $[Ca^{2+}]_i$ responses at high concentrations of econazole in mouse DRG neurons, we first examined the effect of econazole on naïve HEK293 cells (naïve HEK). As shown in Fig. 3 A and B, 30 μM of econazole increased $[Ca^{2+}]_i$ in naïve HEK, and this effect was not eliminated by the removal of extracellular Ca^{2+}. These results suggested that econazole at 10 μM did not increase $[Ca^{2+}]_i$, but at 30 μM, it triggered $[Ca^{2+}]_i$ responses through Ca^{2+} release from intracellular stores in naïve HEK.

Next, we measured the $[Ca^{2+}]_i$ responses to econazole in TRPA1-HEK cells. Econazole at 10 μM evoked $[Ca^{2+}]_i$ increases in TRPA1-HEK cells, as determined by the responsiveness to AITC (Fig. 3C). In contrast, econazole had no effect on the cells expressing TRPV1. Econazole dose-dependently increased $[Ca^{2+}]_i$ in TRPA1-HEK cells (Fig. 3D). As mentioned earlier, econazole induced nonspecific $[Ca^{2+}]_i$ increases at concentrations exceeding 30 μM in naïve HEK. These results clearly indicated that econazole could activate TRPA1.

Effect of miconazole on $[Ca^{2+}]_i$ in mouse DRG neurons and heterologous TRPA1-expressing cells

We also examined the $[Ca^{2+}]_i$ responses to miconazole, which is a structurally related antifungal drug to econazole [2, 27], in mouse DRG neurons. At concentrations of >3 μM, miconazole increased $[Ca^{2+}]_i$ in a concentration-dependent manner. At a high concentration (100 μM), miconazole triggered nonspecific $[Ca^{2+}]_i$ responses and suppressed KCl responses (Fig. 4A). Removal of extracellular Ca^{2+} reduced the $[Ca^{2+}]_i$ responses to miconazole (Fig. 4B). Of the mouse DRG neurons that responded to 10 μM of miconazole (n=30), those that responded to AITC alone, capsaicin alone, both, or neither were 30% (n=9), 13.3% (n=4), 20% (n=6), and 36.7% (n=11), respectively (Fig. 4C). The TRPA1 blocker significantly inhibited the responses to miconazole at 10 μM but not at 30 μM, whereas no inhibition was observed with the TRPV1 blocker (Fig. 4D). Moreover, the responses to 10 μM of miconazole were significantly lower in $TRPA1^{(-/-)}$ mouse DRG neurons than in wild type neurons (Fig. 4E). There were no differences in the $[Ca^{2+}]_i$ responses to miconazole between the wild type and $TRPV1^{(-/-)}$ mouse DRG neurons.

Miconazole increased $[Ca^{2+}]_i$ in naïve HEK cells (Fig. 5A). After removal of extracellular Ca^{2+}, the responses to miconazole at 10 μM were mitigated but were only partially attenuated at 30 μM (Fig. 5B). Miconazole increased $[Ca^{2+}]_i$ in TRPA1-HEK but not in TRPV1-HEK cells (Fig. 5C). The concentration–response relationship of the $[Ca^{2+}]_i$ responses to miconazole was significantly more pronounced in TRPA1-HEK than in naïve HEK cells (Fig. 5D).

These results suggested that miconazole activated TRPA1, although less pronounced than that induced by econazole in mouse DRG neurons.

Effect of fluconazole on mouse DRG neurons and HEK 293 cells with heterologous expression of TRPA1

Unlike the imidazole antifungals econazole and miconazole, fluconazole belongs to the triazole class of antifungals. Fluconazole did not increase $[Ca^{2+}]_i$ in mouse DRG

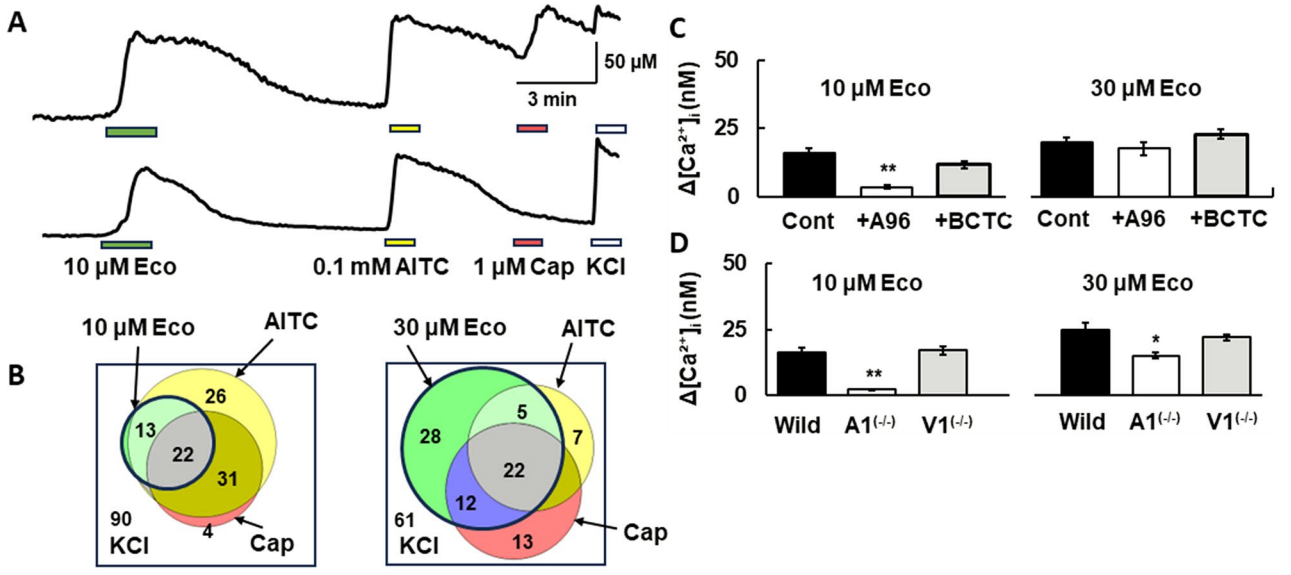

Fig. 2 The $[Ca^{2+}]_i$ responses to econazole and effects of TRP channel antagonists and gene deletion in mouse DRG neurons. (**A**) The actual recordings of $[Ca^{2+}]_i$ responses to the sequential application of 10 μM econazole (Eco), 0.1 mM AITC, 1 μM capsaicin (Cap), and 80 mM KCl are shown. (**B**) The Venn diagrams of the number of neurons that responded to each stimulation with econazole at 10 μM (left) and 30 μM (right). The outer area of all the circles indicates the number of neurons that responded to KCl alone. The data are derived from three mice. (**C**) A summary of $[Ca^{2+}]_i$ responses to econazole at 10 μM (left) and 30 μM (right) in the absence (control) or presence of 10 μM A967079 (A96) or 1 μM BCTC is shown. Columns with vertical lines represent the mean values ± SEM (10 μM econazole: $n = 158–293$, 30 μM econazole: $n = 265–321$ from four mice). $^{**}P < 0.01$ vs. control, one-way ANOVA with Tukey–Kramer test. (**D**) A summary of $[Ca^{2+}]_i$ responses to econazole at 10 μM (left) and 30 μM (right) in wild type (Wild), TRPA1 knockout ($A1^{(-/-)}$), and TRPV1 knockout ($V1^{(-/-)}$) mouse DRG neurons is shown. Columns with vertical lines show the mean values ± SEM (10 μM econazole: wild, $n = 305$; $A1^{(-/-)}$, $n = 280$; $V1^{(-/-)}$, $n = 310$ from four mice. 30 μM econazole: wild, $n = 250$; $A1^{(-/-)}$, $n = 291$; $V1^{(-/-)}$, $n = 171$ from four mice). $^{*}P < 0.05$, $^{**}P < 0.01$ vs. wild, one-way ANOVA with Tukey–Kramer test

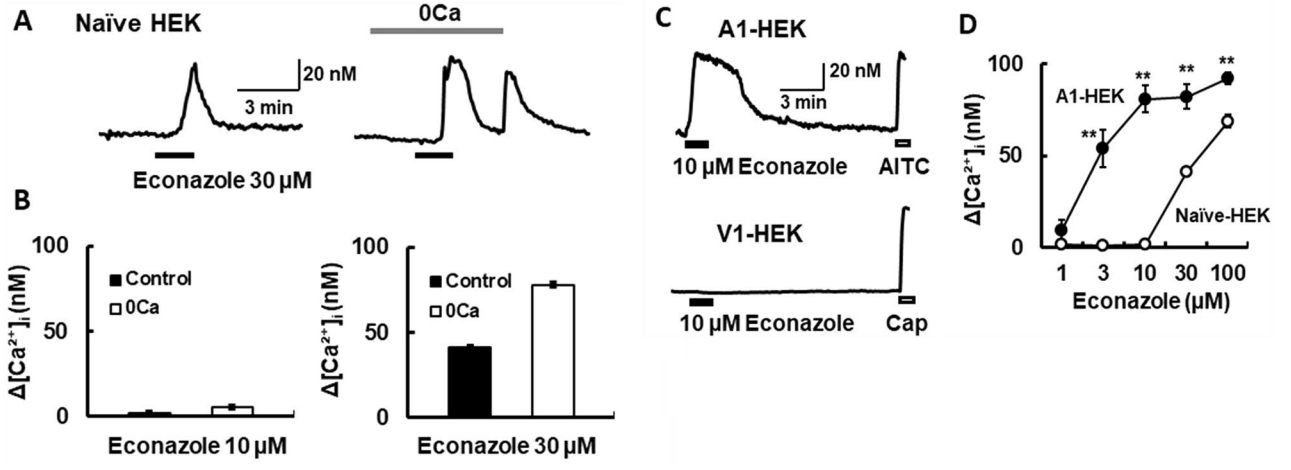

Fig. 3 $[Ca^{2+}]_i$ responses to econazole in naïve and TRPA1-expessed HEK 293 cells. (**A**) The actual recordings of $[Ca^{2+}]_i$ responses to 30 μM econazole in naïve HEK293 cells (naïve HEK) in the presence (left) or absence of external Ca^{2+} (0Ca) (right) are shown. The 0Ca period is indicated with a grayish bar. (**B**) A summary of the amplitudes of $[Ca^{2+}]_i$ responses to econazole at 10 μM (left) and 30 μM (right) in naïve HEK293 cells in the presence (control) or absence of extracellular Ca^{2+} (0Ca) is shown. Columns with vertical lines represent mean ± SEM (10 μM: control, $n = 362$; 0Ca, $n = 278$ from four experiments; 30 μM: control, $n = 390$; 0Ca, $n = 340$ from four experiments). (**C**) The actual recording of $[Ca^{2+}]_i$ responses to 10 μM econazole in HEK293 cells expressing TRPA1 (upper, A1-HEK) and TRPV1 (lower, V1-HEK) is shown. The cells are stimulated by each selective agonist (100 μM AITC and 1 μM Cap). (**D**) The relationship between $[Ca^{2+}]_i$ responses and the concentrations of econazole in A1-HEK and naïve HEK cells is shown. Symbols with vertical lines represent mean ± SEM (A1-HEK, $n = 302–420$; naïve HEK, $n = 150–165$ from four experiments). $^{**}P < 0.01$ vs. naïve HEK, as determined by Student's t-test

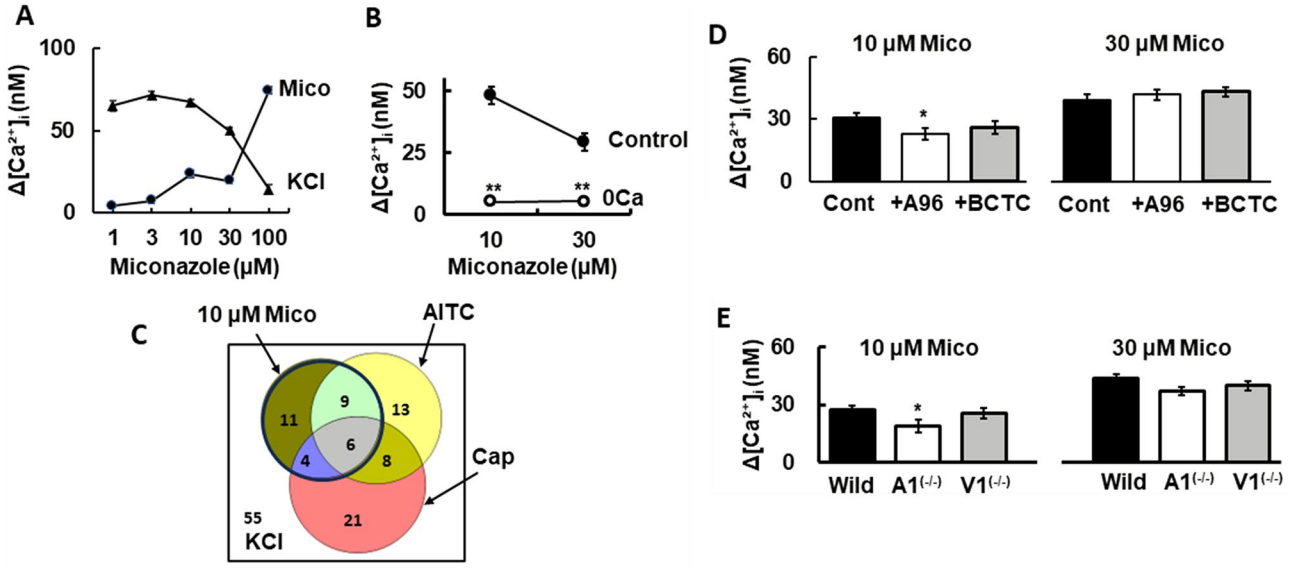

Fig. 4 The $[Ca^{2+}]_i$ responses to miconazole and effects of TRP channel antagonists and gene deletion in mouse DRG neurons. (**A**) The relationship between the magnitude of $[Ca^{2+}]_i$ increase induced by miconazole (Mico) and by KCl at different concentrations of miconazole. Symbols with vertical lines represent mean ± SEM ($n = 132–231$ from 3–6 mice). (**B**) A summary of the amplitudes of $[Ca^{2+}]_i$ responses to 10 and 30 μM of miconazole in the presence (control) and absence of extracellular Ca^{2+} (0Ca) is shown (10 μM: control, $n = 103$; 0Ca, $n = 127$; 30 μM: control, $n = 106$; 0Ca, $n = 93$ from three mice). Some vertical lines are obscured by symbols. (**C**) The Venn diagram shows the number of neurons that responded to 10 μM miconazole (Mico), 0.1 μM AITC, 1 μM capsaicin (Cap), and 80 mM KCl. The outer area of all the circles indicates the number of neurons that responded to KCl alone. Data are from three mice. (**D**) A summary of $[Ca^{2+}]$i responses to miconazole at 10 μM (left) and 30 μM (right) in the absence (Cont) or presence of 10 μM A967079 (A96) or 1 μM BCTC is shown. Columns with vertical lines represent the mean values ± SEM (10 μM miconazole, $n = 120–201$; 30 μM miconazole, $n = 142–199$ from four mice). $^{**}P < 0.01$ vs. control, one-way ANOVA with Tukey–Kramer test. (**E**) A summary of $[Ca^{2+}]_i$ responses to miconazole at 10 μM (left) and 30 μM (right) in wild type (Wild), TRPA1 knockout ($A1^{(-/-)}$), and TRPV1 knockout ($V1^{(-/-)}$) mouse DRG neurons is shown. Columns with vertical lines show the mean values ± SEM (10 μM miconazole: wild, $n = 215$; $A1^{(-/-)}$, $n = 201$; $V1^{(-/-)}$, $n = 198$ from four mice. 30 μM miconazole: wild, $n = 223$; $A1^{(-/-)}$, $n = 198$; $V1^{(-/-)}$, $n = 220$ from four mice). $^{*}P < 0.05$ vs. wild, one-way ANOVA with Tukey–Kramer test

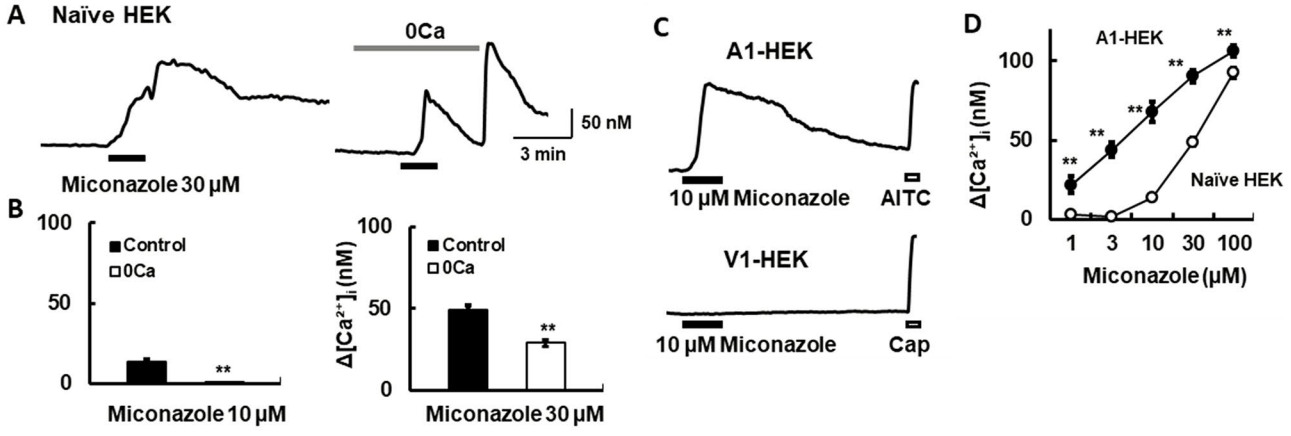

Fig. 5 $[Ca^{2+}]_i$ responses to miconazole in naïve and TRPA1-expessed HEK 293 cells. (**A**) The actual recordings of $[Ca^{2+}]_i$ responses to 30 μM miconazole in the presence (left) or absence of extracellular Ca^{2+} (0Ca) (right) in naïve HEK 293 cells are shown. The 0Ca period is indicated with a grayish bar. (**B**) A summary of the amplitudes of $[Ca^{2+}]_i$ responses to miconazole at 10 μM (left) and 30 μM (right) in naïve-HEK cells in the presence (control) or absence (0Ca) of extracellular Ca^{2+} is shown. Columns with vertical lines represent the mean ± SEM (miconazole 10 μM: control, $n = 103$; 0Ca, $n = 127$; miconazole 30 μM: control, $n = 106$; 0Ca, $n = 93$ from three experiments). $^{**}P < 0.01$ vs. control, as determined by Student's t-test (**C**) The actual recordings of $[Ca^{2+}]_i$ responses to 10 μM miconazole and 100 μM AITC in TRPA1-expressed HEK293 cells (upper, A1-HEK) and to 1 μM capsaicin (Cap) in TRPV1-expressed HEK cells (lower, V1-HEK) are shown. (**D**) The relationship between $[Ca^{2+}]_i$ responses and the concentrations of miconazole in A1-HEK and naïve HEK cells is shown. Symbols with vertical lines represent the mean ± SEM (A1-HEK, $n = 54–134$; naïve-HEK, $n = 298–333$ from 3–4 experiments). $^{**}P < 0.01$ vs. naïve-HEK, as determined by Student's t-test

neurons, even at a concentration of 100 μM, regardless of the expression of TRPA1 and/or TRPV1 (Fig. 6A). Furthermore, $[Ca^{2+}]_i$ responses were not observed when fluconazole (100 μM) was applied to TRPA1-HEK and TRPV1-HEK cells (Fig. 6B). These data showed that TRPA1 and TRPV1 were not activated by fluconazole.

Involvement of TRPA1 in econazole-induced itch and pain

Finally, to examine that econazole actually elicited itch and pain in mice, econazole was intradermally injected into the cheeks of wild type and TRPA1$^{(-/-)}$ mice, and subsequent scratching and wiping behaviors were counted. Econazole induced scratching and wiping behaviors in wild type mice, but the time course of these reactions differed among animals (Fig. 7A, B). The total number of 30-minute behaviors was significantly greater in the econazole-injected group than in the vehicle-injected one. In contrast, the number of both behaviors was significantly lower in TRPA1$^{(-/-)}$ mice than in wild type mice. Since scratching and wiping behavior reflect itch and pain behavior, respectively [21, 22], these data suggest that econazole causes itch and pain in mice through the activation of TRPA1.

Discussion

Econazole is a broad-spectrum antifungal drug that is used for various diseases, such as dermatomycosis. However, its typical adverse effect of skin irritation often hinders effective utilization [1, 2]. In this present study, we aimed to elucidate the mechanisms of econazole-induced irritation by investigating its effects on sensory neurons. Econazole-induced behavioral responses were

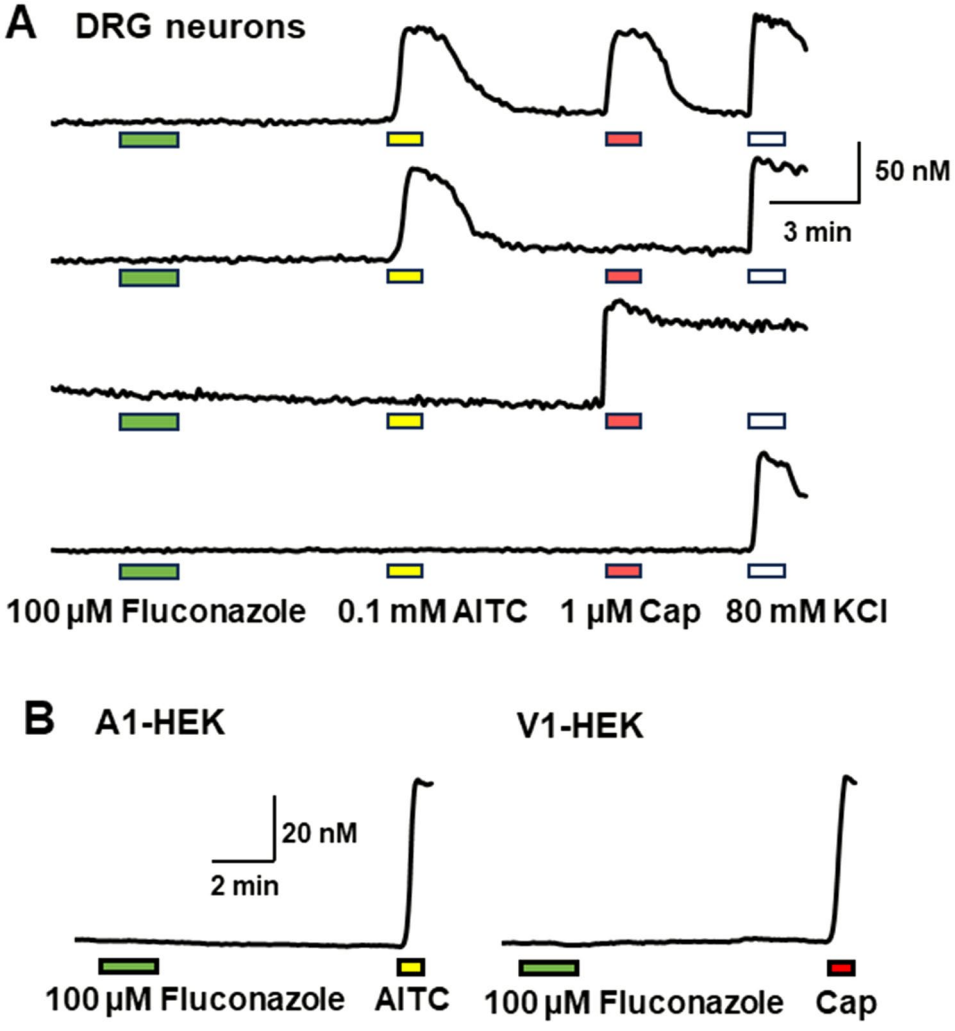

Fig. 6 $[Ca^{2+}]_i$ responses to fluconazole in mouse DRG neurons and HEK293 cells expressing TRPA1. (**A**) The actual recordings of $[Ca^{2+}]_i$ responses to the sequential application of 100 μM fluconazole, 0.1 mM AITC, 1 μM capsaicin (Cap), and 80 mM KCl in mouse DRG neurons depict four patterns of responses. (**B**) The representative changes in $[Ca^{2+}]_i$ induced by 100 μM fluconazole in HEK293 cells expressing TRPA1 (left: A1-HEK) and TRPV1 (right: V1-HEK). To determine the expression of each channel, a specific agonist was applied as follows: 0.1 mM ATIC for TRPA1 and 1 μM capsaicin (Cap) for TRPV1. Similar results are obtained in the two additional experiments

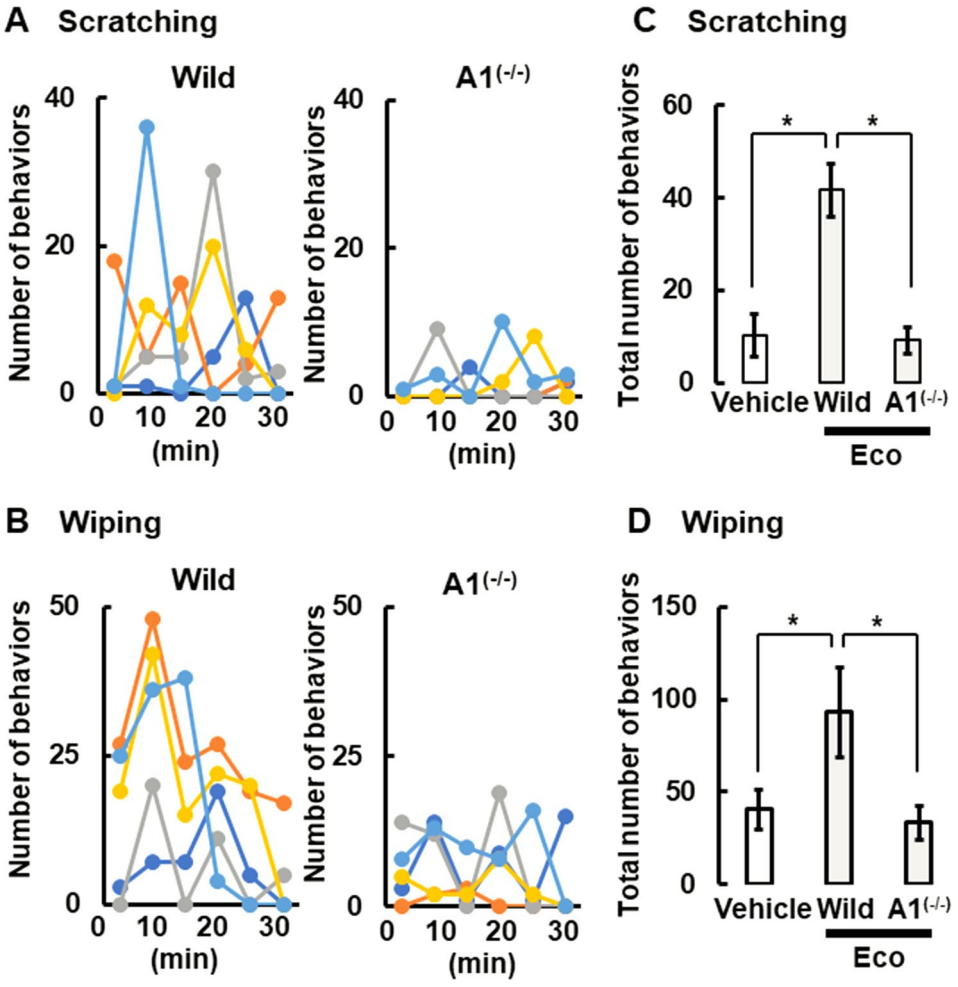

Fig. 7 Econazole induces scratching and wiping behaviors in mice. (**A**, **B**) The time courses of scratching (**A**) and wiping behaviors (**B**) every 5 min for 30 min after the intradermal injection of econazole (50 nmol/10 µl per site) into the right cheeks of wild type (Wild) and TPA1 knockout ($A1^{(-/-)}$) mice. (**C**, **D**) Total number of scratching (**C**) and wiping behaviors (**D**) induced by econazole (Eco) during 30 min in wild type and $TRPA1^{(-/-)}$ mice. Vehicle was administrated into wild type mice. Columns with vertical lines represent mean ± SEM for 4 mice per group. *$P < 0.05$, with Steel-Dwass test

also determined. Moreover, we examined the effects of miconazole, which is a structural analog of imidazole antifungal drugs, and fluconazole, which is a triazole antifungal drug.

Econazole dose-dependently increased the $[Ca^{2+}]_i$ in mouse DRG neurons. At 100 µM, nearly all neurons responded and inhibited KCl-induced responses. Consequently, high concentrations of econazole may exhibit nonspecific actions and potentially cause cellular damage in mouse DRG neurons. Indeed, econazole has been documented to be cytotoxic in various cell types and holds promise as a potential antitumor drug. In one study, econazole increased the lethality of rat thymocytes [28]. In ADR breast cancer cells, econazole reduced cell proliferation and induced strong toxicity, including apoptosis [29]. Furthermore, econazole significantly decreased the viability of human prostate cancer PC3 cells [30]. Similarly, our results showed that miconazole appeared to exert cytotoxic effects (Fig. 4A), consistent with the results of previous studies [31, 32].

Econazole at concentrations of 10 and 30 µM increased $[Ca^{2+}]_i$, and these effects were mitigated upon removal of extracellular Ca^{2+}. Furthermore, nearly all DRG neurons that responded to econazole at 10 µM were found to be sensitive to AITC, suggesting the potential activation of TRPA1 by econazole. The econazole-induced increase in $[Ca^{2+}]_i$ was significantly attenuated by a TRPA1 antagonist; and in $TRPA1^{(-/-)}$ mouse DRG neurons, the $[Ca^{2+}]_i$ responses to econazole were substantially reduced. Moreover, econazole at 10 µM activated the heterologously expressed TRPA1. While econazole exceeding 30 µM induced $[Ca^{2+}]_i$ release in naïve HEK, consistent with previous reports [33, 34]. These findings supported the conclusion that econazole stimulated TRPA1 activation. Topical econazole cream or powder is typically administered as 1% nitric acid, with approximately 10%

penetrating through the stratum corneum [35, 36]. Moreover, econazole applied at 1% to human skin has been reported to be estimated 20 μg/ml (equivalent to 44.9 μM) in epidermal tissue [37]. Therefore, the doses used in clinical practice may be sufficient to activate TRPA1. In contrast, its cytotoxicity may not occur at clinical concentrations, since it does not appear to reach concentrations above 100 μM (Figs. 1C and 4A).

Some of the neurons that responded to econazole also exhibited sensitivity to capsaicin. However, we did not obtain direct evidence on the action of econazole on TRPV1 in HEK 293 cells (Fig. 3C) and this was consistent with the results of a previous report [34]. Notably, econazole at 30 μM partially increased the $[Ca^{2+}]_i$ in TRPA1$^{(-/-)}$ mouse DRG neurons. The $[Ca^{2+}]_i$ responses to this concentration of econazole may be attributed to the Ca^{2+} influx through other channels, as evidenced by the reduced response upon extracellular Ca^{2+} removal. Previous studies have indicated that econazole-induced Ca^{2+} influx can be attenuated by La^{3+} in MDCK cells [38] and by L-type calcium channel blockers in human PC3 cells [30]. Recent report shows that store-operated Ca^{2+} entry, extracellular signaling pathway (ERK) 1/2, protein kinase C and phospholipase A2 are involved in the $[Ca^{2+}]_i$ responses to econazole in human oral cancer cell lines [39]. Therefore, it is suggested that econazole may stimulate many molecules in addition to TRPA1 identified in this study. Since TRPA function is regulated by PKC [40], indirect action via PKC may also be involved in TRPA1 activation by econazole. The nonspecific $[Ca^{2+}]_i$ increases in naïve HEK cells were not abolished by the removal of extracellular Ca^{2+}. It has been reported that econazole induces Ca^{2+} mobilization from intracellular Ca^{2+} stores, similar to thapsigargin, an endoplasmic reticulum Ca^{2+}-ATPase inhibitor [30, 34, 38]. Therefore, this mechanism was considered to elicit in the present study.

The profile of miconazole-induced increase in $[Ca^{2+}]_i$ closely resembled that of econazole in wild type mouse DRG neurons. Miconazole elicited Ca^{2+} influx in neurons that were insensitive to AITC and capsaicin. Notably, the use of a TRPA1 antagonist reduced the miconazole-induced responses. Furthermore, the $[Ca^{2+}]_i$ increases induced by miconazole at 10 μM but not at 30 μM were diminished in TRPA1$^{(-/-)}$ mouse DRG neurons. Intriguingly, miconazole triggered the activation of TRPA1 when expressed in HEK 293 cells. This suggests that miconazole may affect other molecules involved in Ca^{2+} influx more than TRPA1 in mouse DRG neurons. Consequently, unlike econazole, miconazole may possess the capability to activate multiple targets, including TRPA1. Chemical structure of miconazole differs from econazole in terms of the additional single chlorine atom (Fig. 1). The stronger antifungal activity of miconazole than econazole [27, 41] may explain the distinct activities of these molecules. These differences could be helpful in further elucidating the mechanisms of TRPA1 activation.

In general, TRPA1 agonists can be categorized as electrophile or nonelectrophile compounds [8, 42]. Econazole and miconazole belong to the nonelectrophile compound category. The anti-inflammatory drug fenamic acid, which is also classified as a nonelectrophile, has been suggested to activate TRPA1 through protein modification and allosteric binding [14]. These compounds generate reactive oxygen species in the cytosol [42], thereby, indirectly leading to TRPA1 activation [43]. Moreover, econazole is recognized as an inhibitor of TRPM2 channels [44, 45] that contributes to the pathogenesis of inflammatory and neuropathic pain [46]. Similarly, fenamic acid inhibits TRPM2 [44]. There may be a common structural element contributing to the similar effects of econazole and fenamic acid on both TRPA1 and TRPM2. In addition, among TRP channels, econazole has also been reported to inhibit TRPV5 [47] and TRPV6 [48].

Fluconazole, even at a concentration of 100 μM, failed to induce any $[Ca^{2+}]_i$ response in mouse DRG neurons and HEK cells expressing TRPA1 and TRPV1. The structural differences between fluconazole and econazole/miconazole are considerably significant (Fig. 1). Moreover, compared with imidazole compounds, fluconazole has less ability to produce reactive oxygen species, antifungal activity, and cytotoxicity [49]. In contrast, econazole is known to induce apoptosis in certain cell types [50–52]. Therefore, caution should be exercised when using econazole in experiments, because it exerts diverse effects on various cell functions, including TRPA1 activation and TRPM2 inhibition.

Finally, to examine whether econazole elicits itch and pain. the mouse cheek injection model was used. Intradermally injection of econazole into the cheeks elicited scratching and wiping behaviors in wild type mice, but significantly less in TRPA1$^{(-/-)}$ mice. Scratching behaviors reflect itch, while wiping behaviors indicate pain [21, 22]. These results suggested that econazole actually induced adverse effects; itch and pain, in mice through the activation of TRPA1.

In summary, econazole acts as an activator of TRPA1 in sensory neurons, resulting in skin irritation. Blocking TRPA1 activation may offer a potential strategy to mitigate the skin adverse effects induced by econazole.

Abbreviations

AITC	Allyl isothiocyanate
ANOVA	Analysis of variance
Cap	Capsaicin
$[Ca^{2+}]_i$	Intracellular Ca^{2+} concentration
DMSO	Dimethyl sulfoxide
DRG	Dorsal root ganglia
DW	Distilled water
HEK 293	Human embryonic kidney 293

HEPES	N-2-hydroxyethyl-piperazine-2-ethanonesufonic acid
PBS	Phosphate-buffered saline
TRPA1	Transient receptor potential ankyrin 1
TRPV1	Transient receptor potential vanilloid 1
TRPA1-HEK	HEK293 cells expressing TRPA1

Author contributions
T.O. designed the study. K.K. and M.H. conducted the experiments. K.K., K.T., and T.O. conducted data analyses and wrote the manuscript.

Funding
This work was supported, in whole or partly, by the JSPS KAKENHI (Grant No. JP22K06001 to TO).

Data availability
No datasets were generated or analysed during the current study.

Declarations

Ethics approval and consent to participate
This study makes use of mice, and the experimental protocol for the use of animals was approved (Approved number: 21-T-8) by the Committee on Animal Experimentation of Tottori University, Tottori, Japan. No specific consent was needed for the current investigation. All methods were performed following the relevant guidelines and regulations.

Consent for publication
Not applicable.

Competing interests
The authors declare no competing interests.

Received: 2 December 2023 / Accepted: 12 August 2024
Published online: 21 August 2024

References

1. Heel RC, Brogden RN, Speight TM, Avery GS. Econazole: a review of its antifungal activity and therapeutic efficacy. Drugs. 1978;16:177–201.
2. Firooz A, Nafisi S, Maibach HI. Novel drug delivery strategies for improving econazole antifungal action. Int J Pharm. 2015;495:599–607.
3. Moore C, Gupta R, Jordt SE, Chen Y, Liedtke WB. Regulation of pain and itch by TRP channels. Neurosci Bull. 2018;34:120–42.
4. Dai Y. TRPs and pain. Semin Immunopathol. 2016;38:277–91.
5. Gees M, Colsoul B, Nilius B. The role of transient receptor potential cation channels in Ca^{2+} signaling. Cold Spring Harb Perspect Biol. 2010;2:a003962.
6. Jardín I, López JJ, Diez R, Sánchez-Collado J, Cantonero C, Albarrán L, Woodard GE, Redondo PC, Salido GM, Smani T, Rosado JA. TRPs in pain sensation. Front Physiol. 2017;8:392.
7. Zhang H, Wang C, Zhang K, Kamau PM, Luo A, Tian L, Lai R. The role of TRPA1 channels in thermosensation. Cell Insight. 2022;1:100059.
8. Talavera K, Startek JB, Alvarez-Collazo J, Boonen B, Alpizar YA, Sanchez A, Naert R, Nilius B. Mammalian transient receptor potential TRPA1 channels: from structure to disease. Physiol Rev. 2020;100:725–803.
9. Caterina MJ, Leffler A, Malmberg AB, Martin WJ, Trafton J, Petersen-Zeitz KR, Koltzenburg M, Basbaum AI, Julius D. Impaired nociception and pain sensation in mice lacking the capsaicin receptor. Science. 2000;288:306–13.
10. Tominaga M. Nociception and TRP channels. Handb Exp Pharmacol. 2007;179:489–505.
11. Leffler A, Fischer MJ, Rehner D, Kienel S, Kistner K, Sauer SK, Gavva NR, Reeh PW, Nau C. The vanilloid receptor TRPV1 is activated and sensitized by local anesthetics in rodent sensory neurons. J Clin Invest. 2008;118:763–76.
12. Leffler A, Lattrell A, Kronewald S, Niedermirtl F, Nau C. Activation of TRPA1 by membrane permeable local anesthetics. Mol Pain. 2011;7:62.
13. Guinamard R, Simard C, Del Negro C. Flufenamic acid as an ion channel modulator. Pharmacol Ther. 2013;138:272–84.
14. Hu H, Tian J, Zhu Y, Wang C, Xiao R, Herz JM, Wood JD, Zhu MX. Activation of TRPA1 channels by fenamate nonsteroidal anti-inflammatory drugs. Pflugers Arch. 2010;459:579–92.
15. Liu DJ, Collaku A, Dosik JS. Skin irritation and sensitization potential of fixed-dose combination of diclofenac 1% and menthol 3% topical gel: results of two phase I patch studies. Drug Res (Stuttg). 2017;67:119–26.
16. Fischer MJ, Leffler A, Niedermirtl F, Kistner K, Eberhardt M, Reeh PW, Nau C. The general anesthetic propofol excites nociceptors by activating TRPV1 and TRPA1 rather than $GABA_A$ receptors. J Biol Chem. 2010;285:34781–92.
17. Yin S, Luo J, Qian A, Du J, Yang Q, Zhou S, Yu W, Du G, Clark RB, Walters ET, Carlton SM, Hu H. Retinoids activate the irritant receptor TRPV1 and produce sensory hypersensitivity. J Clin Invest. 2013;123:3941–51.
18. Shimada T, Takahashi K, Tominaga M, Ohta T. Identification of molecular targets for toxic action by persulfate, an industrial sulfur compound. Neurotoxicology. 2019;72:29–37.
19. Ohta T, Imagawa T, Ito S. Novel gating and sensitizing mechanism of capsaicin receptor (TRPV1): tonic inhibitory regulation of extracellular sodium through the external protonation sites on TRPV1. J Biol Chem. 2008;283:9377–87.
20. Grynkiewicz G, Poenie M, Tsien RY. A new generation of Ca^{2+} indicators with greatly improved fluorescence properties. J Biol Chem. 1985;260:3440–50.
21. Kittaka H, Uchida K, Fukuta N, Tominaga M. Lysophosphatidic acid-induced itch is mediated by signalling of LPA5 receptor, phospholipase D and TRPA1/TRPV1. J Physiol. 2017;595:2681–98.
22. Yamanoi Y, Kittaka H, Tominaga M. Cheek Injection Model for Simultaneous Measurement of Pain and Itch-related behaviors. J Vis Exp. 2019;151.
23. Mickle AD, Shepherd AJ, Mohapatra DP. Nociceptive TRP channels: sensory detectors and transducers in multiple pain pathologies. Pharmaceuticals (Basel). 2016;9:72.
24. Thastrup O, Cullen PJ, Drøbak BK, Hanley MR, Dawson AP. Thapsigargin, a tumor promoter, discharges intracellular Ca^{2+} stores by specific inhibition of the endoplasmic reticulum Ca^{2+}-ATPase. Proc Natl Acad Sci U S A. 1990;87:2466–70.
25. Gordon-Shaag A, Zagotta WN, Gordon SE. Mechanism of Ca^{2+}-dependent desensitization in TRP channels. Channels. 2008;2:125–9.
26. Gouin O, L'Herondelle K, Lebonvallet N, Le Gall-Ianotto C, Sakka M, Buhé V, Plée-Gautier E, Carré JL, Lefeuvre L, Misery L, Le Garrec R. TRPV1 and TRPA1 in cutaneous neurogenic and chronic inflammation: pro-inflammatory response induced by their activation and their sensitization. Protein Cell. 2017;8:644–61.
27. Hu Z, Zhang J, Cheng X. Antifungal efficiency of miconazole and econazole and the interaction with transport protein: a comparative study. Pharm Biol. 2015;53:251–61.
28. Matsui H, Sakanashi Y, Oyama TM, Oyama Y, Yokota S, Ishida S, Okano Y, Oyama TB, Nishimura Y. Imidazole antifungals, but not triazole antifungals, increase membrane Zn^{2+} permeability in rat thymocytes: possible contribution to their cytotoxicity. Toxicology. 2008;248:142–50.
29. Dong C, Chen Y, Ma J, Yang R, Li H, Liu R, You D, Luo C, Li H, Yang S, Ke K, Lin MC, Chen C. Econazole nitrate reversed the resistance of breast cancer cells to adriamycin through inhibiting the PI3K/AKT signaling pathway. Am J Cancer Res. 2020;10:263–74.
30. Huang JK, Liu CS, Chou CT, Liu SI, Hsu SS, Chang HT, Hsieh CH, Chang CH, Chen WC, Jan CR. Effects of econazole on Ca^{2+} levels in and the growth of human prostate cancer PC3 cells. Clin Exp Pharmacol Physiol. 2005;32:735–41.
31. Jung HJ, Seo I, Jha BK, Suh SI, Baek WK. Miconazole induces autophagic death in glioblastoma cells via reactive oxygen species-mediated endoplasmic reticulum stress Oncol let. 2021;21:335.
32. Lam PL, Wong MM, Hung LK, Yung LH, Tang JC, Lam KH, Chung PY, Wong WY, Ho YW, Wong RS, Gambari R, Chui CH. Miconazole and terbinafine induced reactive oxygen species accumulation and topical toxicity in human keratinocytes. Drug Chem Toxicol. 2022;45:834–8.
33. Chang HT, Liu CS, Chou CT, Hsieh CH, Chang CH, Chen WC, Liu SI, Hsu SS, Chen JS, Jiann BP, Huang JK, Jan CR. Econazole induces increases in free intracellular Ca^{2+} concentrations in human osteosarcoma cells. Hum Exp Toxicol. 2005;24:453–8.
34. Mathivanan S, de la Torre-Martinez R, Wolf C, Mangano G, Polenzani L, Milanese C, Ferrer-Montiel A. Effect of econazole and benzydamine on sensory neurons in culture. J Physiol Pharmacol. 2016;67:851–8.
35. Plempel M. Pharmacokinetics of imidazole antimycotics. Postgrad Med J. 1979;55:662–6.
36. Hänel H, Raether W, Dittmar W. Evaluation of fungicidal action in vitro and in a skin model considering the influence of penetration kinetics of various standard antimycotics. Ann N Y Acad Sci. 1988;544:329–37.

37. Schaefer H, Stüttgen G. Absolute concentrations of an antimycotic agent, econazole, in the human skin after local application. Arzneimittelforschung. 1976;26:432–5.
38. Jan CR, Ho CM, Wu SN, Tseng CJ. Multiple effects of econazole on calcium signaling: depletion of thapsigargin-sensitive calcium store, activation of extracellular calcium influx, and inhibition of capacitative calcium entry. Biochim Biophys Acta. 1999;1448:533–42.
39. Wang JL, Jan CR, Chen MH. Action of econazole on Ca^{2+} levels and cytotoxicity in OC2 human oral cancer cells. J Dent Sci. 2023;18:1280–7.
40. Sánchez JC, Muñoz LV, Galindo-Márquez ML, Valencia-Vásquez A, García AM. Paclitaxel regulates TRPA1 function and expression through PKA and PKC. Neurochem Res. 2023;48:295–304.
41. Qin F, Wang Q, Zhang C, Fang C, Zhang L, Chen H, Zhang M, Cheng F. Efficacy of antifungal drugs in the treatment of vulvovaginal candidiasis: a bayesian network meta-analysis. Infect Drug Resist. 2018;11:1893–901.
42. Macpherson LJ, Dubin AE, Evans MJ, Marr F, Schultz PG, Cravatt BF, Patapoutian A. Noxious compounds activate TRPA1 ion channels through covalent modification of cysteines. Nature. 2007;445:541–5.
43. Viana F. TRPA1 channels: molecular sentinels of cellular stress and tissue damage. J Physiol. 2016;594:4151–69.
44. Chen GL, Zeng B, Eastmond S, Elsenussi SE, Boa AN, Xu SZ. Pharmacological comparison of novel synthetic fenamate analogues with econazole and 2-APB on the inhibition of TRPM2 channels. Br J Pharmacol. 2012;167:1232–43.
45. Hill K, McNulty S, Randall AD. Inhibition of TRPM2 channels by the antifungal agents clotrimazole and econazole. Naunyn Schmiedebergs Arch Pharmacol. 2004;370:227–37.
46. Haraguchi K, Kawamoto A, Isami K, Maeda S, Kusano A, Asakura K, Shirakawa H, Mori Y, Nakagawa T, Kaneko S. TRPM2 contributes to inflammatory and neuropathic pain through the aggravation of pronociceptive inflammatory responses in mice. J Neurosci. 2012;32:3931–41.
47. Hughes TET, Lodowski DT, Huynh KW, Yazici A, Del Rosario J, Kapoor A, Basak S, Samanta A, Han X, Chakrapani S, Zhou ZH, Filizola M, Rohacs T, Han S, Moiseenkova-Bell VY. Structural basis of TRPV5 channel inhibition by econazole revealed by cryo-EM. Nat Struct Mol Biol. 2018;25:53–60.
48. Neuberger A, Nadezhdin KD, Sobolevsky AI. Structural mechanisms of TRPV6 inhibition by ruthenium red and econazole. Nat Commun. 2021;12:6284.
49. Kobayashi D, Kondo K, Uehara N, Otokozawa S, Tsuji N, Yagihashi A, Watanabe N. Endogenous reactive oxygen species is an important mediator of miconazole antifungal effect. Antimicrob Agents Chemother. 2002;46:3113–7.
50. Choi EK, Park EJ, Phan TT, Kim HD, Hoe KL, Kim DU. Econazole induces p53-dependent apoptosis and decreases metastasis ability in gastric cancer cells. Biomol Ther (Seoul). 2020;28:370–9.
51. Ho YS, Wu CH, Chou HM, Wang YJ, Tseng H, Chen CH, Chen LC, Lee CH, Lin SY. Molecular mechanisms of econazole-induced toxicity on human colon cancer cells: G0/G1 cell cycle arrest and caspase 8-independent apoptotic signaling pathways. Food Chem Toxicol. 2005;43:1483–95.
52. Dong C, Yang R, Li H, Ke K, Luo C, Yang F, Shi XN, Zhu Y, Liu X, Wong MH, Lin G, Wang X, Leung KS, Kung HF, Chen C, Lin MC. Econazole nitrate inhibits PI3K activity and promotes apoptosis in lung cancer cells. Sci Rep. 2017;7:17987.

Publisher's Note